Analysis of ultra-broadband high-energy optical parametric chirped pulse amplifier based on YCOB crystal

Meizhi Sun (孙美智)[1*], Lailin Ji (季来林)[2], Qunyu Bi (毕群玉)[1], Nannan Wang (王楠楠)[1], Jun Kang (康 俊)[1], Xinglong Xie (谢兴龙)[1], Zunqi Lin (林尊琪)[1]

[1]*National Laboratory on High Power Laser Physics, Shanghai Institute of Optics and Fine Mechanics, Chinese Academy of Sciences, Shanghai 201800, China*

[2]*Shanghai Institute of Laser plasmas, Chinese Academy of Engineering Physics, Shanghai 201800, China*

[*]*Corresponding author: eric913@mail.ustc.edu.cn*

Received March 9, 2011; accepted April 21, 2011; posted online July 11, 2011

A new type of optical parametric chirped pulse amplifier is designed and analyzed for the amplification of pulse centered at 808 nm. A novel crystal, yttrium calcium oxyborate $YCa_4O(BO_3)_3$ (YCOB), is utilized in the power amplification stage of optical parametric amplification (OPA). Noncollinear phase matching parameters in the *xoz* principle plane of YCOB, compared with those in BBO and DKDP, are analyzed by numerical simulation. The results show that YCOB rather than DKDP can be used in the power amplification stage of OPA to realize the amplification of chirped pulse to several joules with a gain bandwidth exceeding 100 nm. This can be used to gain a high intensity pulse of ∼10 fs after the compressor.

OCIS codes: 190.4410, 190.4970, 140.4480.
doi: 10.3788/COL201109.101901.

The amplification of the femtosecond pulse is an important branch of ultra-intense laser technology, with Ti: sapphire as the medium for its large gain bandwidth. From the perspective of technical features and applications, such femtosecond pulses are used to study high field physics and other related areas in ultrashort time[1,2]; however, the pursuit of higher energy femtosecond pulse should not be abandoned. Optical parametric chirped pulse amplification (OPCPA) has been successfully used in the front end of high intensity lasers[3−8], indicating the possibility of femtosecond pulse amplification. This has been verified by an increasing number of fine crystals being invented, such as $YCa_4O(BO_3)_3$ (YCOB)[9−12].

In contrast with the nonlinear crystals commonly utilized in high energy OPCPA systems, YCOB crystal possesses several prominent properties, including high fracture strength, moderate thermal conductivity and nonlinear coupling, and damage threshold of as high as 1 GW/cm^2 at 532 nm[12,13]. Refractive indexes and transmission spectra of YCOB crystal have been reported in Ref. [12]. In particular, the growth of YCOB to 7.5 (diameter) ×25 (length) (cm) boule has been scaled[14,15], that is, the available YCOB aperture is much larger than those of LiB_3O_5 (LBO) and $Ba(BO_2)_2$ (BBO), which are currently limited to 2 cm. Most studies on the nonlinearity of YCOB crystal during the 1990s focused on the second and the third harmonic generation[11]. In recent years, it has been successfully employed in the power amplification stage of OPCPA as pre-amplification of some PW lasers centered around 1 058 nm[15]. In 2006, Chekhlov *et al.* reported their OPCPA system, in which the output energy of the signal pulse is centered at 1 050 nm and up to 35 J and pulse bandwidth of 84 fs are achieved with pump pulse of 190 J from the second harmonic of the Vulcan laser; in addition, the large aperture crystal in the power amplification is KH_2PO_4 (KDP)[16]. To the best of our knowledge, YCOB has not been used in OPCPA systems centered at 808 nm to achieve output energy of up to several joules and pulse width of ∼10 fs.

In the current study, a new type of OPCPA to amplify pulse of ∼10 fs up to several joules is analyzed, and YCOB rather than KDP or KD_2DO_4 (DKDP) crystal is applied as the gain medium of power amplification stage. This is because YCOB with nonlinear coefficient that is four times larger than those of KDP and DKDP can provide a broad enough gain bandwidth. The system consisted of five parts: the signal pulse laser, Öffner stretcher, optical parametric amplifier, compressor, and the pump pulse lasers (Fig. 1). The oscillator provided signal pulses of 10-fs time duration and 2 nJ in energy. The signal pulses are chirped to 15 ps/nm by an eight-pass Öffner stretcher with 10% transmission efficiency, and chirped signal pulse energy injected into the optical parametric amplification (OPA) chain is 0.2 nJ. The OPA consisted of two stages. The first stage was the pre-amplification, including 3 pieces of BBO crystals that offer the majority of the system gain. The pump pulses at 532 nm with 300 mJ of energy for the first 2 pieces of BBO crystals were provided by a commercial single longitudinal mode Nd: YAG pump laser. For the third piece of the BBO crystal, 5% second harmonic generation of uncompressed output pulse of upgraded subpicosecond laser system (SPS) was utilized as the pump pulse[17]. In the second stage, a piece of YCOB crystal with a large aperture (∼50 mm) was employed as the gain medium, and the SPS provided the pulse at 526.5 nm with the desired special-temporal shape and energy exceeding 50 J. The signal was amplified in the *xoz* principle plane of YCOB because the effective nonlinear coefficient (d_{eff}) in the *xoz* principle plane was much larger than those in the *xoz* and *yoz* principle planes[18,19].

Noncollinear geometric configuration with type-1

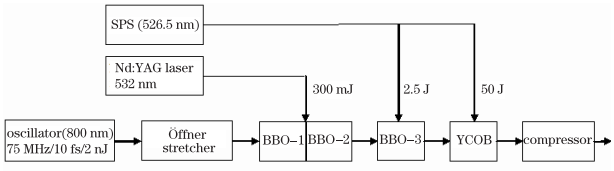

Fig. 1. Optical schematic layout of the OPCPA.

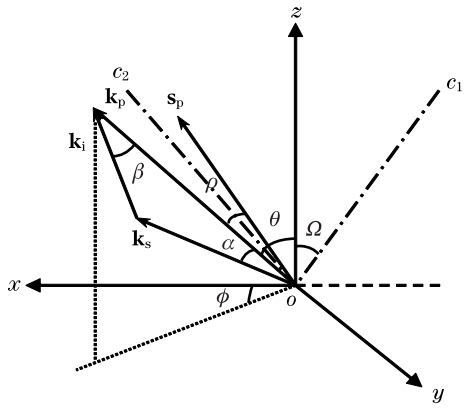

Fig. 2. Noncollinear phase matching vectors in biaxial crystals.

phase matching o+o→e is generally adopted in all OPA stages. Compared with the collinear geometric configuration, the noncollinear geometric configuration can achieve larger parametric bandwidth and obtain higher conversion efficiency by compensating for the walk-off effects of the pump pulse with non-collinear angle. The wave vectors and parameters of the noncollinear phase matching in biaxial crystals are shown in Fig. 2. The refractive indexes along the principal axis are ordered as follows: $n_z > n_y > n_x$. Moreover, c_1 and c_2 are optical axises, Ω is the optic axial angle, Φ is the azimuth of $\mathbf{k}_\mathrm{p}$ in xoz principle plane, and $\mathbf{k}_\mathrm{s}$, $\mathbf{k}_\mathrm{i}$, and $\mathbf{k}_\mathrm{p}$ are the wave vectors of the signal, idle, and pump, respectively. The symbol α refers to the noncollinear angle, θ is the phase matching angle, ρ is the walk-off angle, $\mathbf{s}_\mathrm{p}$ is the Poynting vector of pump pulse, and β is the angle between $\mathbf{k}_\mathrm{i}$ and $\mathbf{k}_\mathrm{p}$. Momentum conservation and energy conservation during OPA can be expressed as

$$\mathbf{k}_\mathrm{p} = \mathbf{k}_\mathrm{i} + \mathbf{k}_\mathrm{s}, \tag{1}$$

$$\omega_\mathrm{p} = \omega_\mathrm{i} + \omega_\mathrm{s}. \tag{2}$$

The wave vector mismatch is expressed as

$$\Delta k = k_\mathrm{p} - k_\mathrm{s}\cos\alpha - k_\mathrm{i}\cos\beta. \tag{3}$$

The optimized noncollinear configuration can realize the highest parametric bandwidth ($\Delta\lambda_p$) for the ultrabroadband optical parametric amplifier. Generally, the noncollinear angle in such a configuration is set to realize group velocity matching (GVM) between the signal and pump pulses[20]. However, according to numerical analysis, there is a small difference between the GVM noncollinear angle and the one realizing the highest parametric bandwidth[21]. In the present paper, parametric bandwidths as well as gain bandwidths ($\Delta\lambda_g$) and acceptance angles ($\Delta\theta$) were calculated according to the definitions but not the approximation of Taylor series. In addition, an identical analytic method was adopted from Ref. [19].

Parametric bandwidth is defined as the interval of the signal wave length, which restricts the phase mismatching smaller than $\pm\pi$, under the condition that perfect phase matching is achieved at the center wavelength of OPA. It can be expressed as $|\Delta kL| \leqslant \pi$, where L is the crystal length. Figure 3 (a) shows the curves of the parametric bandwidths against noncollinear angles in 15-mm BBO, 15-mm YCOB, and 35-mm DKDP crystals. Parametric bandwidths of 149.6 and 108 nm were achieved in YCOB and BBO when the noncollinear angles were 2.763°and 2.358°, respectively (Fig. 3(a)). However, the value was 46 nm in DKDP when the noncollinear angle was 3.821°. Parametric bandwidth is consistent with the gain bandwidth to a large extent. Gain bandwidth is defined as the interval of the signal wave length, which restricts the gain that is bigger than half of that achieved at the center wavelength of the signal pulse. However, numerical analysis indicated a little difference (Fig. 3); specifically, the largest gain bandwidth of 133.6 nm was achieved at a noncollinear angle of 2.775° in YCOB, 112.4 nm at 2.345° in BBO, and 46.6 nm at 3.819° in DKDP. As a conclusion, the gain bandwidths of YCOB and BBO were broad enough for the amplification of chirped pulses in the system, while DKDP was restricted to the amplification of chirped pulses with original pulse duration exceeding 21 fs at 808 nm.

The walk-off effect results from the separation of the Poynting and wave vectors of light transmitting in

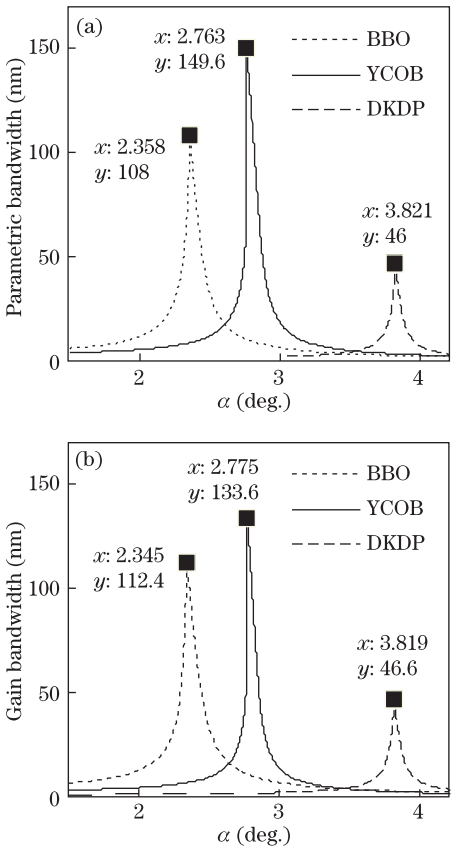

Fig. 3. (a) Parametric bandwidth and (b) gain bandwidth versus noncollinear angles in BBO (dotted line), in the xoz principle plane of YCOB (solid line), and in DKDP (dashed line).

Table 1. Noncollinear Phase Matching Parameters of BBO, YCOB, and DKDP

	α (deg.)	$\theta_{\rm pm}$ (deg.)	$\Delta\lambda_p$ (nm)	$d_{\rm eff}$ (pm/V)	ρ (deg.)	$\Delta\theta$ (deg.)	$\Delta\lambda_g$ (nm)	$I_{\rm p}$ (GW/cm^2)	L (m)
BBO-1/2	2.345	23.78	108	2.096	–3.288	0.0214	112.4	0.4	0.015
BBO-3	2.4	23.86	132	2.095	–3.295	0.0214	127	0.4	0.015
YCOB	2.775	(26.4,180)	149.6	0.935	1.134	0.0599	133.6	0.5	0.015
DKDP	3.819	52.76	46	0.295	–2.913	0.0113	46.6	2	0.035

nonlinear crystals (inhomogeneous medium). This leads to spatial displacement between the signal and pump pulses as well as the degradation of conversion efficiency in OPA. Furthermore, the walk-off effect plays an important role in the impact of wavefront phase distortion of pump on the beam quality of signal in OPA[22,23]. The acceptance angle is defined as the interval of θ, which restricts the wave vector mismatch that is smaller than $\pm\pi$/L around the perfect phase matching angle $\theta_{\rm pm}$ at 808 nm. A large acceptance angle means a stable OPA. The walk-off, acceptance, and phase matching angles versus non-collinear angles are shown in Fig. 4. Corresponding to the optimal noncollinear angle, the walk-off angle in YCOB crystal was 1.134°, the acceptance angle was ∼0.06°, and the phase matching angle was 26.4°. The values of BBO and DKDP are enumerated in Table 1. Based on the results, YCOB possessed a larger acceptance angle and smaller walk-off angle than BBO and DKDP.

For chirped signal pulse pumped by 532-nm Gaussian shaped pulse at intensity ($I_{\rm p}$) of 0.4 GW/cm^2 in 15-mm BBO crystal, a gain of 2 372 is realized (Fig. 5(a)). In the initial two pieces of BBO crystal in the pre-amplification stage, the unsaturated gain of 1 000 for each piece was achieved by pumping with 532-nm pulse of 300 mJ at an intensity of 0.4 GW/cm^2, and the signal pulse energy was 0.2 mJ. In the third piece of BBO crystal, the injected signal pulse was amplified by 526.5-nm 10 th order super-Gaussian shaped pump pulse, of which the energy was 2.5 J at an intensity of 0.4 GW/cm^2. The phase matching parameters listed in Table 1 are calculated with the same method. The results were not very different from those pumped by pulse at 532 nm. The BBO crystal employed in this stage had a 13 (aperture)×15 (length) (mm) in realizing the saturated gain of ∼2 000 so that energy of signal pulse was amplified up to ∼0.4 J. The majority of energy was provided by the second stage. Figure 5(b) shows the gain curve in the *xoz* principle plane of YCOB with a 526.5-nm pump pulse. For the YCOB crystal with a 15-mm length, saturated gain of ∼20 was realized with pump pulse at an intensity of 0.5 GW/cm^2 and energy of 50 J. In the power amplification stage, signal pulse of ∼8 J was achieved with broad spectrum bandwidth. Furthermore, saturated amplification in both stages greatly improved the stability of the system[24]. In contrast, normalized gain curve in 35-mm DKDP is shown in Fig. 5(a) when pumped by 526.5-nm pulse at intensity of 2 GW/cm^2. DKDP is an excellent choice for amplification of pulse centered at 808 nm with original time duration exceeding 20 fs.

The compressor consisted of a pair of gratings and a piece of reflector. They were arranged in tandem in a four-pass configuration with a Littrow incident angle of 36.3° to match the stretcher; this was ensured so as to

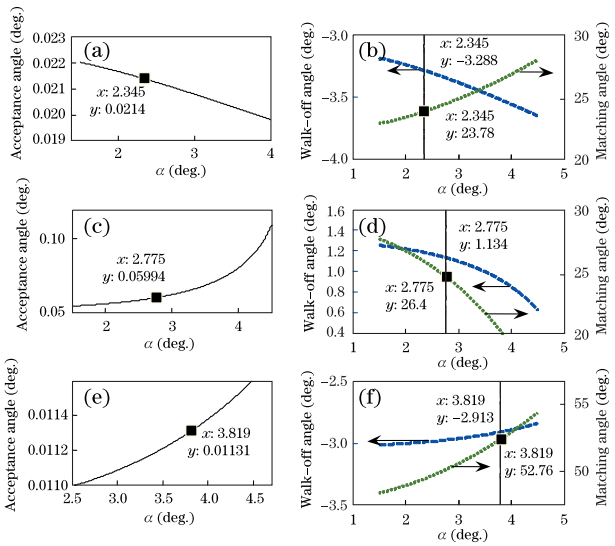

Fig. 4. Acceptance angle (solid line), walk-off angle (dashed line), and phase matching angle (dotted line) versus non-collinear angle in (a)(b) BBO, (c)(d) the *xoz* principle plane of YCOB, and (e)(f) DKDP.

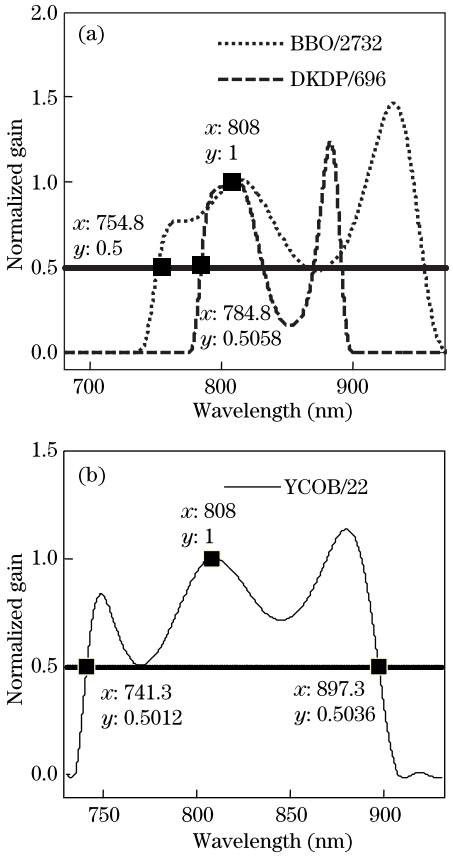

Fig. 5. Normalized gain curves in (a) BBO (dotted line) and DKDP (dashed line); (b) *xoz* principle plane of YCOB crystal (solid line).

compress the chirped pulse to Fourier transform limitation. The transmission efficiency of the compressor was ∼75%, and the energy of output ultra-short pulse was ∼6 J.

In conclusion, a new type of OPCPA system to realize the amplification of pulse centered at 808 nm is analyzed. The noncollinear phase matching parameters of YCOB are compared with those of BBO and DKDP in detail. Numerical analysis shows that YCOB, rather than DKDP, can be utilized to amplify ultra-broadband chirped pulse so as to compress the signal pulse to ∼10 fs after the compressor. With YCOB as the gain medium of power amplification stage of OPCPA, a total gain of $\sim 4\times10^{10}$ is achieved, with the energy of the amplified signal pulse up to several joules.

This work was supported by the National "863" Program of China under Grant No. 2009AA8044010.

References

1. P. Hansheng, Chinese J. Lasers (in Chinese) **33,** 721 (2006).
2. A. Dubietis, G. Jonusauskas, and A. Piskarskas, Opt. Commun. **88,** 437 (1992).
3. I. N. Ross, P. Matousek, M. Towrie, A. J. Langley, and J. L. Collier, Opt. Commun. **144,** 125 (1997).
4. I. N. Ross, P. Matousek, G. H. C. New, and K. Osvay, J. Opt. Soc. Am. B **19,** 2945 (2002).
5. E. Hugonnot, G. Deschaseaux, O. Hartmann, N. Beck, and H. Coïc, in *Proceedings of OSA Technical Digest Series* (CD) MB4 (2007).
6. M. Sun, J. Kang, A. Guo, F. Zhang, Q. Yang, Q. Bi, X. Xie, and Z. Lin, Acta Opt. Sin. (in Chinese) **30,** 1234 (2010).
7. Y. Kitagawa, H. Fujita, R. Kodama, H. Yoshida, S. Matsuo, T. Jitsuno, T. Kawasaki, H. Kitamura, T. Kanabe, S. Sakabe, K. Shigemori, N. Miyanage, and Y. Izawa, IEEE J. Quantum Electron. **40,** 281 (2004).
8. C. N. Danson, P. A. Brummitt, R. J. Clarke, J. L. Collier, B. Fell, A. J. Frackiewicz, S. Hancock, S. Hawkes, C. Hernandez-Gomez, P. Holligan, M. H.-R. Hutchinson, A. Kidd, W. J. Lester, I. O. Musgrave, D. Neely, D. R. Neville, P. A. Norreys, D. A. Pepler, C. J. Reason, W. Shaikh, T. B. Winstone, R. W. W. Wyatt, and B. E. Wyborn, Nucl. Fusion **44,** (suppl.) 239 (2004).
9. R. Norrestam, M. Nygren, and J. O. Bovin, Chem. Mater. **4,** 737 (1992).
10. G. Aka, A. Kahn-Harari, F. Mougel, D. Vivien, F. Salin, P. Coquelin, P. Colin, D. Pelenc, and J. P. Damelet, J. Opt. Soc. Am. B **14,** 2238 (1997).
11. Z. Wang, K. Fu, X. Xu, X. Sun, H. Jiang, R. Song, J. Liu, J. Wang, Y. Lin, J. Wei, and Z. Zhao, Appl. Phys. B **72,** 839 (2001).
12. M. Iwai, T. Kobayashi, H. Furuya, Y. Mori, and T. Sasaki, Jpn. J. Appl. Phys. **36,** 276 (1997).
13. C. A. Ebbers, A. J. Bayramian, R. Campbell, R. Cross, B. L. Freitas, Z. Liao, K. I. Schaffers, S. Sutton, J. A. Caird, and C. P. J. Barty, in *Proceedings of Advanced Solid-State Photonics, OSA Technical Digest Series* (CD) (2008).
14. Z. M. Liao, I. Jovanovic, and C. A. Ebbers, Opt. Lett. **36,** 1277 (2006).
15. E. W. Gaul, M. Martinez, J. Blakeney, A. Jochmann, M. Ringuette, D. Hammmond, T. Borger, R. Escamilla, S. Douglas, W. Henderson, G. Dyer, A. Erlandson, R. Gross, J. Caird, C. Ebbers, and T. Ditmire, Appl. Opt. **49,** 1676 (2010).
16. O. V. Chekhlov, J. L. Collier, I. N. Ross, P. K. Bates, M. Notley, C. Hernandez-Gomez, W. Shaikh, C. N. Danson, D. Neely, P. Matousek, S. Hancock, and L. Cardoso, Opt. Lett. **31,** 3665 (2006).
17. X. Xie, J. Zhu, F. Liu, J. Yang, F. Guan, G. Huang, Y. Dai, M. Li, S. Xue, Q. Gao, Z. Xue, M. Shao, Y. Zhang, A. Han, Z. Peng, W. Zhang, M. Zhang, C. Zhu, Z. Lin, Z. Zhang, Y. Ding, J. Chen, S. Wang, Y. Gu, W. Wang, R. Wang, and J. Wu, Chinese J. Lasers (in Chinese) **30,** 865 (2003).
18. Mi. V. Pack, D. J. Armstrong, and A. V. Smith, J. Opt. Soc. Am. B **22,** 417 (2005).
19. M. Sun, Q. Bi, F. Zhang, J. Kang, X. Xie, and Z. Lin, Acta Opt. Sin. (in Chinese) **31,** 0119001 (2011).
20. T. Wilhelm, J. Piel, and E. Riedle, Opt. Lett. **22,** 1494 (1997).
21. J. Wang, J. Yao, F. Li, Y. Yu, and X. Shi, Acta Opt. Sin. (in Chinese) **21,** 139 (2001).
22. F. Zhang, Y. Wang, M. Sun, Q. Bi, X. Xie, and Z. Lin, Chin. Opt. Lett. **8,** 217 (2010).
23. X. Wei, L. Qian, P. Yuan, H. Zhu, and D. Fan, Opt. Express **16,** 8904 (2008).
24. J. Kang, S. Chen, J. Zhu, and H. Wei, Optics & Laser Technology **39,** 1084 (2007).